MS-I

SUMMARY REPORT

1 July 1963 to 15 March 1965
Contract and Control No. NAS8-5431

SENSOR, FUEL DEPLETION

Prepared for

George C. Marshall Space Flight Center
Huntsville, Alabama

DO 5872
March 1965

Prepared by R. W. Remington
R. W. Remington,
Project Engineer

Approved by N E Wood
N. E. Wood,
Director of Engineering

Approved by Joe H. Burson
Technical Supervisor NASA

Acoustica Associates, Inc., 5331 West 104th Street, Los Angeles, California 90045
(213) SPring 6-2610

1.0 INTRODUCTION

This is the summary report, as defined under contract number NAS8-5431 for George C. Marshall Space Flight Center of the National Aeronautics and Space Administration, submitted by Acoustica Associates, Inc. This report covers the period of technical effort from 1 July 1963 through 15 March 1965, and is the summary of Acoustica Associates, Inc. Document DO 5721 and DO 5756 through DO 5756-19.

2.0 ABSTRACT

23209

A detailed description of the control unit and the mode of operation of the four basic sections, oscillator, switch driver, output switch, and wet-dry simulator are discussed along with the radio interference filter, failure mode analysis of the unit and a section on fluid dynamic characteristics of the sensor.

AUTHOR

3.0 OSCILLATOR

The oscillator is a transistorized Hartley type, which is tuned and set to be controlled at its frequency of oscillation by the high Q series notch resonance of a specially designed piezoelectric sensor. The "off" or "on" state of the oscillator is determined by the piezoelectric element being either (1) mass loaded by a liquid of a specific density causing the electrical impedance at resonant frequency (f_r) in the oscillator feedback loop to look high, "off", or (2) the piezoelectric element unloaded, such as when in gas, allowing the electrical impedance at (f_r) in the oscillator feedback loop to look low, "on."

The transistor current gain β and the turns ratio of the feedback transformer windings are the limiting factors in the design of the oscillator. The operating point of the transistor is selected to obtain saturation in collector current, resulting in a partially clipped sinusoidal output.

In carrying out an analysis of the oscillator circuit to establish the range of variables (in particular, the feedback turns ratio and the current gain of the transistor), it is necessary to note that the transistor is a current sensitive device and the circuit configuration must lend itself to supplying the base current requirement. For this reason the feedback circuit comprising secondary of T1 and C2 of schematic 102575, is a series circuit having an idealized impedance at 80 kc, approximating the input impedance of the base circuit of the transistor in parallel with the equivalent bias network (R2 and R7).

Using linear circuit approximations, it may be shown that the condition for oscillation may be expressed to a first approximation in terms of the feedback transformer turns ratio.

$$a = \frac{N_2}{N_1}$$

and the h_{12e} parameter for the transistor is

$$h_{12e} = \frac{1 + 0.96a}{a\,(a + 0.96)}$$

for closely coupled coils and a reasonable load on the feedback winding.

While the result of this expression is only approximate, it does indicate the limits over which h_{12e} may vary and still have a circuit in which the signal currents are oscillatory. It is important that this oscillation criterion be taken into account when considering variation of the transistor parameters with temperature and, hence, oscillator output amplitude variation.

Early in the design of the oscillator and the associated DRY SIMULATE circuit it was found that there was erratic behavior in these circuits at certain times. A general analysis of this erratic behavior disclosed that the difficulty was in the DRY SIMULATE switching circuit composed of Q5 and R8 as related to the characteristics of the oscillator circuit. The entire circuit of the NAF 120 was build up on a special breadboard and caused to exhibit the undesired characteristic. It was shown that the problem was caused by the value of R8 being somewhat lower than might be desired for stable operation of the oscillator during the simulated dry condition. When the value of R8 is too low the oscillator tends to function in two different modes, (1) that characteristic to its normal tuned frequency, and (2) at a much lower frequency, thus producing an output at 80 kc modulated by approximately 2 kc.

When the value of R8 was changed to 1500 ohms, the trouble was completely eliminated.

In normal use of the sensing device, that is, with the sensor crystal circuitry controlling the oscillator, none of the units could be caused to produce an undesired output characteristic.

To verify the operation of this circuit section, exhaustive tests were performed using water, RP-1, and finger loading in an attempt to cause a malfunction. In every case, the oscillator assembly responded as intended, displaying the designed output characteristics.

4.0 SWITCH DRIVER

The driver stage is coupled to the oscillator stage from the low impedance output of the oscillator feedback winding. Since the input impedance of the driver stage is quite low, it is necessary to employ a resistor coupling technique to avoid loading the oscillator while obtaining sufficient base drive to adequately maintain switch driver output with variations of supply voltage and temperature.

The output from the oscillator feedback winding is a clipped sine wave and swings negative with respect to circuit common. Application of this signal to the driver stage results in a square wave output.

The signal is then transformed to a lower voltage at a higher current level and rectified in order to drive the final switching device. The square wave output from the driver is generally the result of this stage being driven to saturation and then to the off state during input reversal time. Operation of the transistor in this manner provides high efficiency since the device is either all off or all on, requiring no power losses as a result of bias levels. A more significant advantage is that full wave rectification of the transformed square wave output makes filter networks and further losses unnecessary. At the frequency of operation, the base to emitter capacitance of the output switching device provides adequate filtering. The rectifying diodes have been chosen to have fast recovery time with minimal forward drop at the required operating frequency and current level.

Since some transformer ringing will occur during off time of the transistor, a capacitor is placed across the primary winding which reduces spike amplitudes to levels well within safe maximum BVceo ratings for the transistor. Further protection against problems due to excessive Vce is provided by the low dc resistance between base and emitter of the device.

5.0 OUTPUT SWITCH

The transistor chosen for this application will provide up to one ampere load switching capability with a resistive load and up to 500 milliamperes load switching with inductive loads. This device is so driven as to allow the load to be placed in either the collector or emitter circuits, however to meet the specification requirements the load is being switched in the emitter circuit allowing the load to be common to the 28 vdc input power line common side. The transistor switch is driven to saturation during on time and is totally off during oscillator off time except for a very small residual current resulting from I_{cbo}. This current is only a few microamperes and does not degrade the operation of the circuit.

The characteristics of the chosen output switching transistor are such that during ON time at one ampere load current Vce (sat) is generally less than 0.6 volts allowing for low power dissipation at maximum load current. Since the device is silicon and is mounted on a heatsink, no injurious junction temperature will be incurred during prolonged operation at one ampere levels and elevated environmental temperatures as dictated by specification requirements.

The output of this switching stage has been protected against inductive voltage peaks by the inclusion of a clipping diode. This ensures reliable operation with inductive loads such as relays or solenoids.

6.0 WET-DRY SIMULATION

Simulation of either wet or dry condition is included in the circuitry and is accomplished at the oscillator through the use of low saturation level transistor switches.

Simulation is accomplished by the application 28 ±4 vdc to the appropriate terminal of either transistor simulation circuit. Wet simulation is provided by switching the oscillator transistor's base to a voltage significantly below the emitter potential thereby cutting the oscillator off. This test function will be operated when the sensor is dry, thus overriding control by the sensor. Dry simulation is achieved through the use of a similar transistor switch. This function is accomplished by bypassing the high impedance of the sensor circuit with the lower impedance of the simulating transistor when it is turned on. This test function will be operated only when the sensor is wet, once again overriding the control of the sensor.

7.0 RADIO INTERFERENCE

The original specification made no provision for prevention of radio frequency interference and for that reason no radio frequency interference filter was included in the design of the sensor. A later specification included testing under MIL-I-6181D.

As a result of tests conducted on December 9, 1963 a radio frequency interference filter was added to the sensor. A new sensor was fabricated with the transformers and filter assembly integrally potted within the housing. While it was possible to fit the filter network into the existing housing dimensions, several mechanical design changes within the housing were necessary.

The new sensor was tested in accordance with MIL-I-6181D. Its performance during certain portions of the tests was not acceptable because of the particular load which was used. When an optional load specified by MIL-I-6181D was employed, the sensor's performance was electrically satisfactory.

Upon proving the filter design adequate, the unit was encapsulated and sealed. Additional tests were performed. These tests included vibration (sinusoidal and randon), shock and radio interference. Schematic drawing 102575 shows the filter design which was incorporated in the system in order to comply with specification MIL-I-6181D on radio frequency interference.

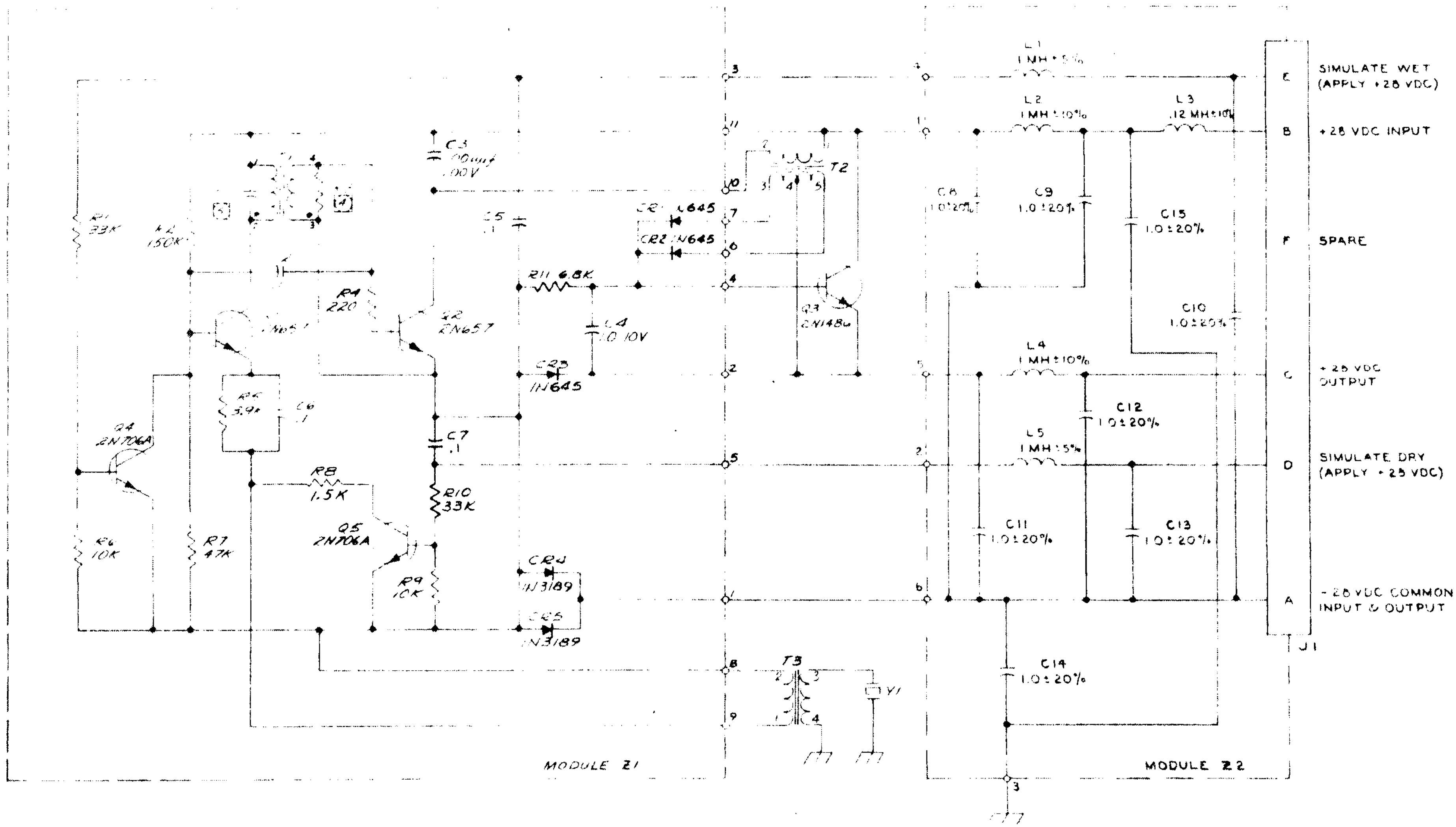

Schematic Drawing 102575

8.0 FAILURE MODE

References

MIL-HDBK-217

Reliability Stress and Failure Rate Data for Electronic Equipment

RELIABILITY FAILURE ANALYSIS

This failure analysis is performed as Part of the Design Review Program for the NAF-120.

With one exception, all failure rate data is computed according to MIL-HDBK-217 Military Standarization Handbook of Reliability Stress and Failure Rate Data for Electronic Equipment published by the Department of Defense.

The exception is the failure rate for lox sensor crystals which was taken from data accumulated at Acoustica Associates, Inc., for the past three (3) years.

DEFINITIONS

R = Reliability: The probability that a system will give satisfactory performance for a given period of time when used in the manner and for the purpose intended.

t = Mission Time: Mission time for this analysis is [illegible] min. (.0852 hour)

F_R = Failure Rate: Number of failures per unit of time, taken from MIL-HDBK-217. (Military Standardization Handbook D. O. D.)

Q = Unreliability = 1-reliability: The probability that the system will fail to give satisfactory performance for a given period of time when used in the manner and for the purpose intended.

SUMMARY

FAILURE MODE

The following results were obtained by the methods shown in the paragraph entitled CALCULATIONS:

The probability of successful operation when sensor is wet is R_W = .9999921

The probability of successful operation when sensor is dry is R_D = .99935?7.

The probability of successful operation when sensor is either wet or dry is R_S = .9993518.

Reliability = 99.93518%

This is equivalent to less than 65 failures out of 100,000 missions.

(Each mission being .0832 hour long).

Assuming these 65 failures were to occur, examination of the Failure Mode indicates the following:

1. The probability of a "DRY" signal when sensor is "WET" = 1.2%
2. The probability of a "WET" signal when sensor is "DRY" = 98.8%

This means, that should a failure occur, there is a 1.2% probability that the failure will be such that the detector will produce a "DRY" signal when a sensor is "WET", and there is 98.8% probability that it will produce a "WET" signal when sensor is "DRY".

EFFECT ANALYSIS

Liquid Oxygen Level Detector

The effect of an erronious dry signal when the sensor is wet, would be the premature indication of a dry signal.

The effect of a wet signal when the sensor is dry, would be the failure to indicate a dry signal.

CALCULATIONS

Probability of success when sensor is dry:

$$R_D = e^{-t \times F_R}$$

When: t = .0832 hour

F_R = Failure Rate for Detector with Dry Sensor

F_R = .0000962/hour (summation of F_R for each component shown in Figure I). x 80*

Then: $R_D = e^{-.0832 \times .0000962 \times 80}$

$= e^{-.0006403}$

R_D = .9993597

* Failure rates are for ground operation. An environment factor of 80 shall be used during Launch Phase.

Probability of success when sensor is wet:

$$R_W = e^{-t \times F_R}$$

When: t = .0832 hour

F_R = Failure Rate for Detector with Wet Sensor

= .00000118/hour (summation of F_R for each component shown in Figure II). x 80*

Then:

$$R_W = e^{-.0832 \times .00000118 \times 80}$$

$$= e^{-.0000079}$$

$$R_W = .9999921$$

Probability of success when sensor is either wet or dry is:

$$R_S = R_D \times R_W$$

$$= .9993597 \times .9999921$$

$$R_S = .9993518$$

FAILURE MODE

Q = Probability of failure when sensor is either wet or dry

= $1-R$ = 1-.9993518

Q = .0006482

Q_W = Probability of failure when sensor is wet

= $1-R_W$ = 1-.9999921

Q_W = .0000079

Q_D = Probability of failure when sensor is dry

= $1-R_D$ = 1-.9993597

Q_D = .0006403

* Failure rates are for ground operation. An environment factor of 80 shall be used during Launch Phase.

In the event of failure then:

The probability of failure when sensor is wet is:

$$q_W = \frac{Q_W \times 100}{Q}$$

$$q_W = \frac{.0000079 \times 100}{.0006482} = 1.2\%$$

And the probability of failure when sensor is dry is:

$$q_d = \frac{Q_D \times 100}{Q}$$

$$q_d = \frac{.0006403 \times 100}{.0006482} = 98.8\%$$

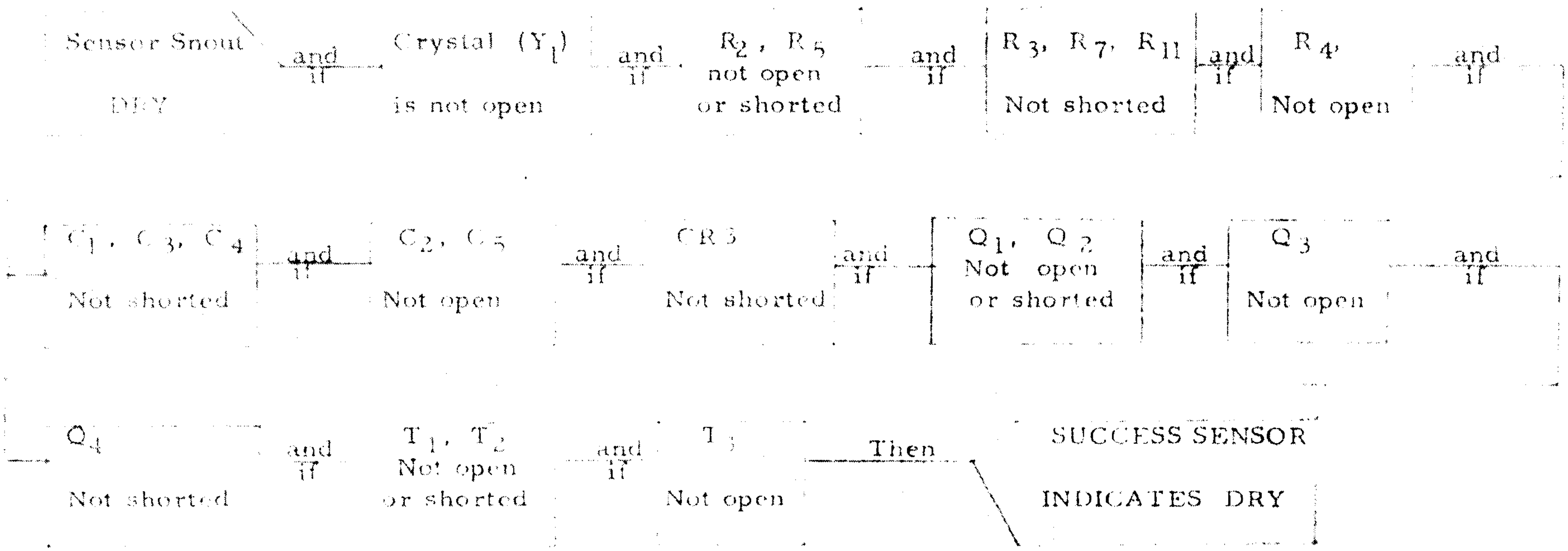

TOTAL FAILURE RATE FOR ABOVE COMPONENTS = 9 62%/1000 HOURS
COMPONENT FAILURE RATES ARE LISTED IN TABLE I

SUCCESS DIAGRAM FOR DRY SENSORS

FIGURE I

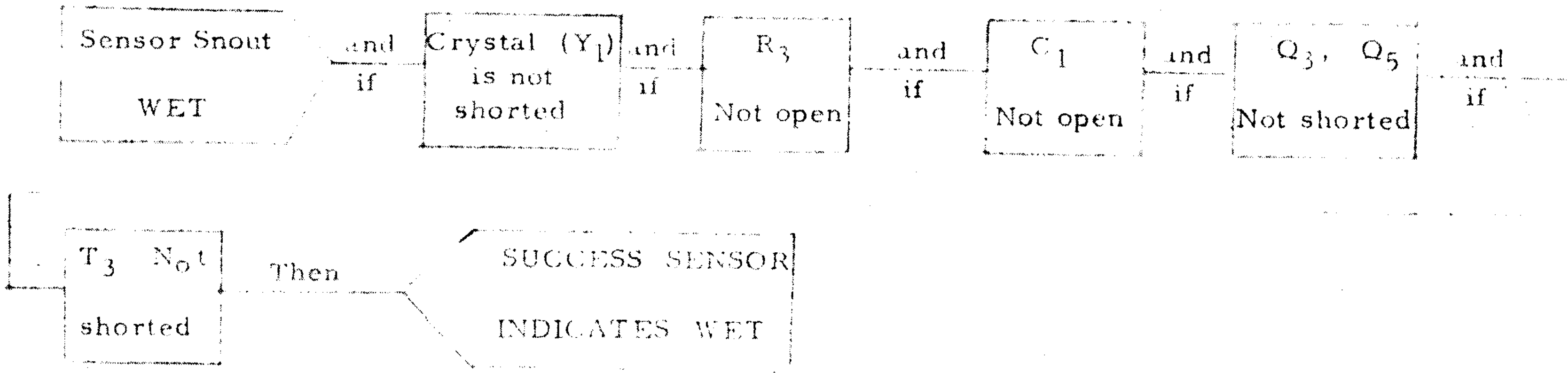

TOTAL FAILURE RATE FOR ABOVE COMPONENTS = .118%/1000 HOURS
COMPONENT FAILURE RATES ARE LISTED IN TABLE I

SUCCESS DIAGRAM FOR WET SENSOR

FIGURE II

TABLE I

Component	Sym.	F_R /1000 Hours	Qty.
Resistors	R_3 - R_9	.023	7
	R_1 & R_{10}	.024	2
	R_2	.028	1
	R_{11}	.039	1
Capacitors	C_1 - C_4 & C_6	.001	5
	C_5 & C_7	.005	2
Diodes	CR_1 & $_2$	.015	2
	CR_3	.020	1
	CR_4 & $_5$	.016	2
Transistors	Q_1, Q_3 & Q_4	.020	3
	Q_2	.021	1
	Q_5	.025	1
Transformers	T_1 - T_3	.050	3
Crystal	Y_1 open	9.200*	1
	Y_1 shorted	0.000	

* Failure rate data for crystals is taken from data accumulated at Acoustica Associates, Inc., on Liquid Oxygen Sensors.

COMPONENT			SENSOR CONDITION		OUTPUT INDICATION		Output Failure
	Failure Mode						
SYM.	Open	Short	WET	DRY	WET	DRY	
R_1	X		X		X		
		X	X		X		
	X			X		X	
		X		X		X	
R_2	X		X		X		
		X	X		X		
	X			X	X		X
		X		X	X		X
R_3	X		X			X	X
		X	X		X		
	X			X		X	
		X		X	X		X
R_4	X		X		X		
		X	X		X		
	X			X	X		X
		X		X		X	
R_5	X		X		X		
		X	X		X		
	X			X	X		X
		X		X	X		X
R_6	X		X		X		
		X	X		X		
	X			X		X	
		X		X		X	

COMPONENT			SENSOR CONDITION		OUTPUT INDICATION		Output Failure
	Failure Mode						
SYM.	Open	Short	WET	DRY	WET	DRY	
R_7	X		X		X		
		X	X		X		
	X			X		X	
		X		X	X		X
R_8	X		X		X		
		X	X		X		
	X			X		X	
		X		X		X	
R_9	X		X		X		
		X	X		X		
	X			X		X	
		X		X		X	
R_{10}	X		X		X		
		X	X		X		
	X			X		X	
		X		X		X	
R_{11}	X		X		X		
		X	X		X		
	X			X		X	
		X		X	X		X
C_1	X		X			X	X
		X	X		X		
	X			X		X	
		X		X	X		X

COMPONENT			SENSOR CONDITION		OUTPUT INDICATION		Output Failure
	Failure Mode						
SYM.	Open	Short	WET	DRY	WET	DRY	
C_2	X		X		X		
		X	X		X		
	X			X	X		X
		X		X		X	
C_3	X		X		X		
		X	X		X		
	X			X		X	
		X		X	X		X
C_4	X		X		X		
		X	X		X		
	X			X		X	
		X		X	X		X
C_5	X		X		X		
		X	X		X		
	X			X		X	
		X		X		X	
C_6	X		X		X		
		X	X		X		
	X			X	X		X
		X		X		X	
C_7	X		X		X		
		X	X		X		
	X			X		X	
		X		X		X	

SYM.	COMPONENT Failure Mode		SENSOR CONDITION		OUTPUT INDICATION		Output Failure
	Open	Short	WET	DRY	WET	DRY	
CR_1	X		X		X		
		X	X		X		
	X			X		X	
		X		X		X	
CR_2	X		X		X		
		X	X		X		
	X			X		X	
		X		X		X	
CR_3	X		X		X		
		X	X		X		
	X			X		X	
		X		X	X		X
CR_4	X		X		X		
		X	X		X		
	X			X		X	
		X		X		X	
CR_5	X		X		X		
		X	X		X		
	X			X		X	
		X		X		X	
Q_1	X		X		X		
		X	X		X		
	X			X	X		X
		X		X	X		X

COMPONENT			SENSOR CONDITION		OUTPUT INDICATION		Output Failure
	Failure Mode						
SYM.	Open	Short	WET	DRY	WET	DRY	
Q_2	X		X		X		
		X	X		X		
	X			X	X		X
		X		X	X		X
Q_3	X		X		X		
		X	X			X	X
	X			X	X		X
		X		X		X	
Q_4	X		X		X		
		X	X		X		
	X			X		X	
		X		X	X		X
Q_5	X		X		X		
		X	X			X	X
	X			X		X	
		X		X		X	
T_1	X		X		X		
		X	X		X		
	X			X	X		X
		X		X	X		X
T_2	X		X		X		
		X	X		X		
	X			X	X		X
		X		X	X		X

COMPONENT			SENSOR CONDITION		OUTPUT INDICATION		Output Failure
	Failure Mode						
SYM.	Open	Short	WET	DRY	WET	DRY	
T_3	X		X		X		
		X	X			X	X
	X			X	X		X
		X		X		X	
Y_1	X		X		X		
		X	X			X	X
	X			X	X		X
		X		X		X	
	X		X				
		X	X				
	X			X			
		X		X			
	X		X				
		X	X				
	X			X			
		X		X			
	X		X				
		X	X				
	X			X			
		X		X			
	X		X				
		X	X				
	X			X			
		X		X			

2.0 FLUID DYNAMICS

A study of fluid dynamic characteristics of sensors immersed in propellants was undertaken to better understand the problem of fluid separation under high velocity conditions. The sensor exhibits different characteristics of separation from various liquids at their liquid-vapor interfaces, and this phenomenon was also investigated. Included in this evaluation were motion picture studies of propellant flow past the sensor at high velocities.

The fluid dynamic characteristics of bodies and fluids are generally coordinated with empirical and theoretical data. The problem areas are not directly associated with the calculations, but with the information concerning the environment and various assumptions required to perform the analysis.

The approaches which will be followed are basically comparative. That is, Reynolds' Number calculation, drag and flow separation determination are the topics of discussion.

To determine if flow separation exists on the surface of a cylindrical sensor body when exposed to normal flow of the propellant.

The assumptions necessary to determine if flow separation is a problem are:

a. Density and temperature of the propellant do not change any more than the allowable flow variations. The specific gravity of fuel was determined at 60°F and used as a constant.

b. Calculations will be performed primarily for steady state flow conditions.

c. The sensor-tank relationship is simulated by a cylinder and flat plate for boundary layer calculations, drag comparisons, etc.

d. Propellant sloshing and wave effects are not taken into account and sufficient pressure gradient exists due to favorable tank configuration in the sensor area (A reduction in area as flow proceeds toward the outlet).

An investigation of the interactions between the fluid dynamic characteristics of the propellant (RP-1) and the sensor position in the tank is part of the installation and performance evaluation of the system. The installation of a sensor probe into a moving fluid environment may provoke the possibility of flow separation around the sensor. Boundary layer, Reynolds' Number, sensor configuration and other physical phenomena are contributing factors to flow separation. Therefore, the analysis presented below is used to determine if flow separation alters the function of the sensor installation.

a. Physical environment of the probe

The sensor probe extends normal to the tank wall and approximately two (2) inches into the propellant tank, measured from the wall of the tank to the tip of the sensor. The propellant flows by the sensor station at a velocity of approximately 36 inches per second, with a tolerance band of plus or minus 2 inches per second. Under these circumstances, the initial investigation determined the Reynolds' Number range of the configuration and installation.

Using the standard Re (Reynolds' Number) equation.

$$Re = 7730 \frac{D'V\rho'}{\mu'}$$

where D' = diameter of sensor, feet

V = propellant velocity, feet per second

ρ' = specific gravity of the propellant relative to water

μ' = viscosity of the propellant, centipoise

$$Re = \frac{7730\,(0.375)\,(36/12)\,(0.810)}{1.5} = 4700$$

In figure 1, Reynolds' Number variations are presented as a function of specific gravity of RP-1. The velocity tolerances of the propellant, namely ±2 inches per second and specific gravity variations in the equation, have little effect upon changing turbulent flow to laminar, thus Reynolds' Number. The Reynolds' Number calculation for this installation indicated

FIGURE I

SPECIFIC GRAVITY AND REYNOLDS' NUMBER

$$R_E = \frac{7230\ D'V'\rho'}{\mu'}$$

WHERE

D' = SENSOR DIA. ~ INCHES
V' = PROPELLANT FLOW VELOCITY ~ FT./SEC.
ρ' = SP. GR. OF THE PROPELLANT RELATIVE TO WATER.
μ' = VISCOSITY ~ CENTIPOISE

ρ' = .810 FOR RP-1
t = 60°F
μ' = 1.5 CENTIPOISE

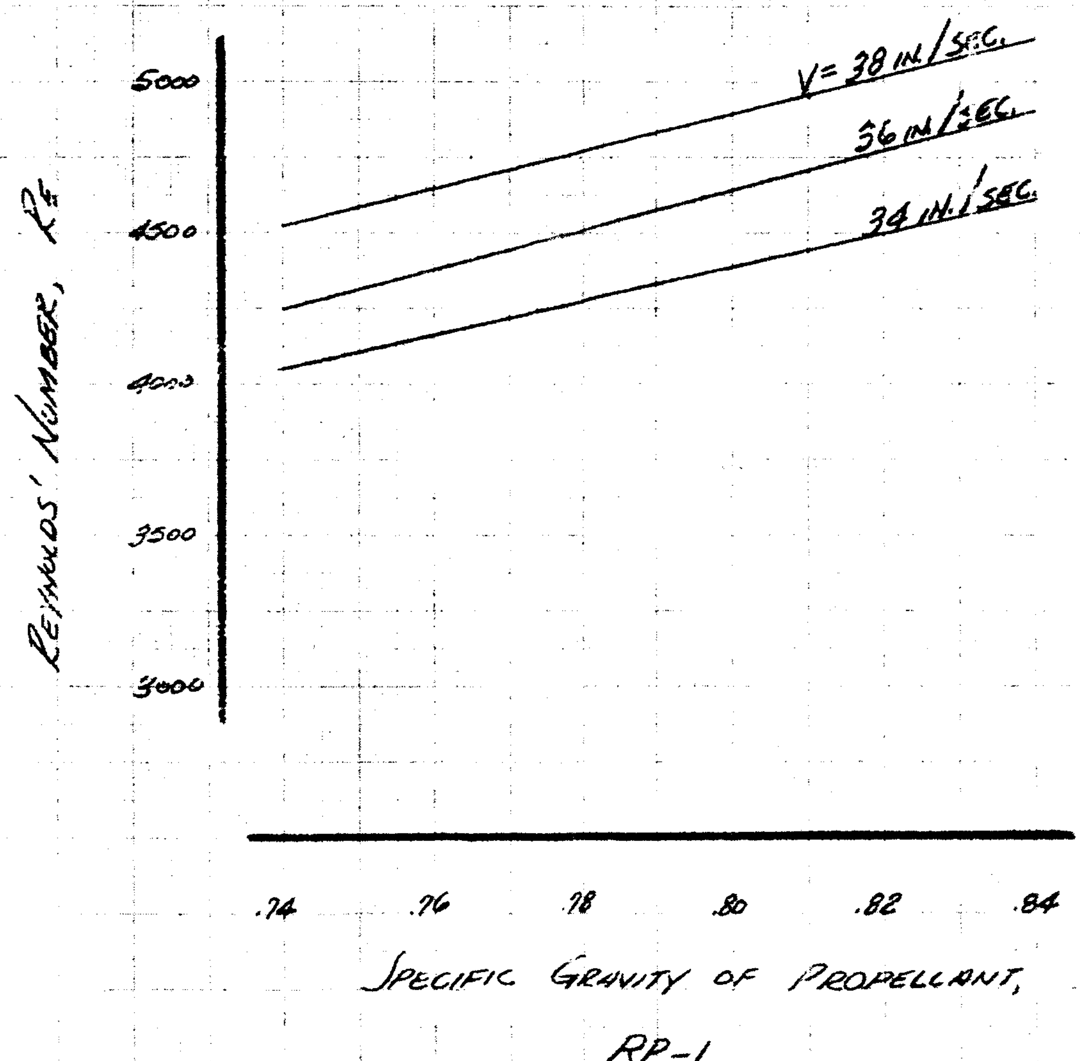

that turbulent flow characteristics will generally be experienced. However, the Reynolds' Number is in the transitional zone and fluctuation between laminar and turbulent flow is a direct possibility of the variables. Fage and Walker conducted laminar flow airfoil tests in a wind tunnel and Steven water tank. The latter is used to determine the Froudes' Number.

The results showed that the same airfoil produced turbulent flow characteristics at a lower Reynolds' Number than results of the wind tunnel. Therefore at the same Reynolds' Number, it is possible to see turbulent flow in water and laminar flow in air for the same configuration.

b. General flow characteristics of the propellant and sensor. The Reynolds' Number describes the fluid interaction characteristics of a cylindrical sensor in the propellant. The drag coefficient, C_D, for a cylinder is

C_D = 1.2 for low Reynolds' Number (laminar flow)

C_D = 1.0 for low-medium Reynolds' Number (turbulent flow).

The difference in C_D is attributable mainly to the separation at the end or tip of the sensor. It also reflects the Reynolds' Number difference.

It can be shown in figure 2 and 3 that drag characteristics are determined from Froudes' Number.

$$C_D = 0.5 + \frac{1}{F_n^2} = 0.5 + \frac{gh}{V^2}$$

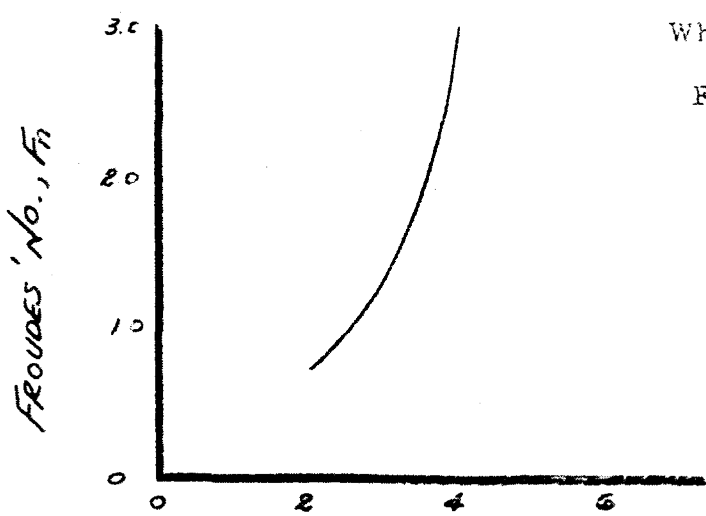

Where V = velocity

F_n = Froudes' No.

= $V/\sqrt{gh}$

g = 32 ft./sec.^{2}

h = distance of the cylinder into the fluid, feet.

FIG. 2 – VELOCITY, V – FT./SEC.

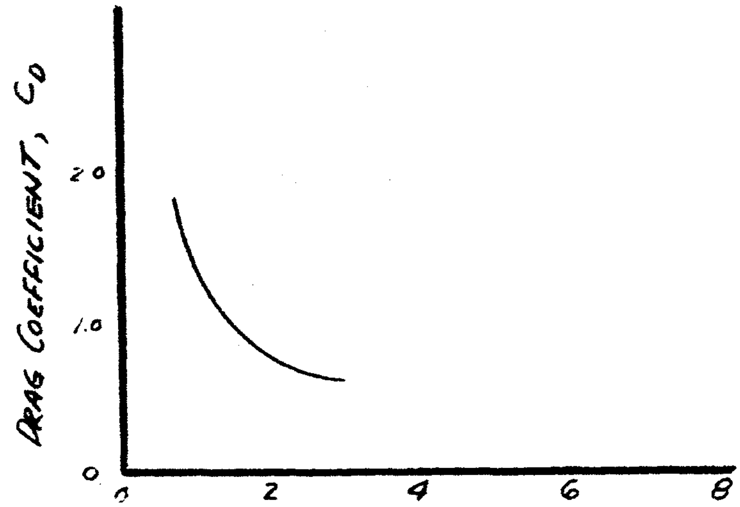

FIG. 3 FROUDE'S No., F_n

In the reference, "Fluid Dynamic Drag." by S. G. Hoerner, the flow separation created by the end or tip of the sensor in the fluid is essentially similar to a phenomenon encompassing pressure coefficients and incipient cavitation for three-dimensional figures. (See figure 4.)

A correlation exists between the pressure and drag coefficients. That is,

$$C_p = \frac{\Delta P}{q} \qquad \text{and} \qquad C_D = \frac{D}{S\,q}$$

where C_p = pressure coefficient

C_D = drag coefficient

ΔP = change in loss in pressure, PSI

q = dynamic pressure on head, PSI

D = drag, lb.

S = drag area, square feet

The combination of D/S is effectively a loss in force in terms of drag over a given area. In other words, Δ P is approximately equal to the parameter D/S. Since incipient cavitation indicates minimum pressure coefficient, it can be shown in figure 4, the relationship of flow separation to pressure coefficient.

The starting point of flow separation is generally instituted at the leading edge or upstream edge of the cylindrical tip of the sensor. Flow separation is a direct function of the propellant flow characteristics and primarily, leading edge profile. The latter will determine whether the flow will generate an adverse pressure peak (negative pressure gradient). If the flow does not separate at the point of discussion, then the pressure profile will gradually recover to a plateau pressure for the remainder of the X/D ratio. In figure 4 the curve with the solid line indicates initial separation and recovery. The curve represented by dash lines indicates separation without recovery.

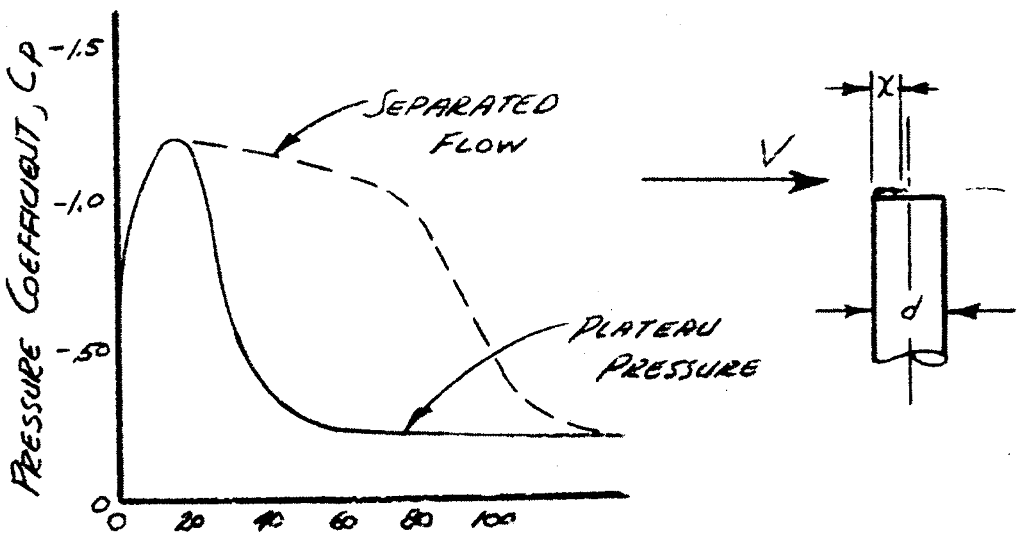

Figure 4. Length Ratio, X/D-%

The separation which shows an adverse pressure peak (negative pressure gradient) gradually recovers to a plateau pressure. The beginning of the plateau pressure is generally located at the heel of the pressure profile. The heel is located at approximately 40 to 50% of X/D where X is the specific location of the plateau pressure and D is the diameter of the cylinder. The point of separation is generally 10 to 20% of X/D, with 15%, being the average. It seems logical to reason that flow separation at the leading edge will exist and that the flow will re-attach. Therefore, no downstream separation will be transmitted from the sensor.

As long as the boundary layer conditions along the tank wall do not intercept the sensor tip, the boundary layer profile per se will not interfere with the function of the sensor tip. It is estimated that the fluid flow velocity passing by the sensor tip is approximately the mid-stream velocity of the fluid. The variation which may affect the performance of the sensor is the eddy or funnel effects of the outlet and its relationship to the tank bottom. However, this may be offset by a more favorable pressure gradient in the sensor locale.

The boundary layer calculation is presented to show that it does not have any effect upon sensor and its location. For turbulent flow characteristics, the seventh power boundary layer profile equation is used.

$$\delta / X = 0.154/Re^{1/7}$$

where δ = boundary layer thickness

X = distance upstream from the station measured, assuming flat plate

Re = Reynolds' Number

$$\delta / X = 0.154/4700^{1/7} = 0.154/3.35$$

$$\delta / X = 0.046$$

The sensor probe extends into the fluid 2 inches. If the boundary layer thickness is assumed as 2 inches, then

$$X = \frac{\delta}{.046} = \frac{2.000}{.046} = 43.5$$

The value of the calculated X, distance upstream from the station measured, is much greater than the installation. The boundary layer build up will not exceed 2 inches at the sensor station. To reiterate, analysis is based upon a flat plate boundary layer effects. Therefore, the sensor tip will feel full mid-stream velocity of the propellant.

The sensor tip and sensor body are a unit made of two different diametrical cylinders. The use of a simple cylindrical shape to calculate various flow characteristics is not altered by the actual configuration for this Reynolds' Number range.

SUMMARY AND CONCLUSION

The following is a summary and conclusion of the events.

1. The Reynolds' Number for this installation generally classifies the flow as turbulent.

2. The flow separation will not be experienced by the sensor tip. If it does, then separation will be a direct function of the Reynolds' Number and configuration profile.

3. The pressure gradient of the sensor-tank environment is favorable when compared to the probable sloshing, eddying and funneling conditions which may exist near the bottom of the tank.

4. There is sufficient evidence by various analogies that the total performance at the sensor in the given environment will perform according to the Acoustica specifications.